Novel acquisition scheme for diffusion kurtosis imaging based on compressed-sensing accelerated DSI yielding superior image quality

Tim Sprenger[1,2], Jonathan I. Sperl[1], Brice Fernandez[3], Vladimir Golkov[1], Ek Tsoon Tan[4], Christopher Hardy[4], Luca Marinelli[4], Michael Czisch[5], Philipp Saemann[5], Axel Haase[2], and Marion I. Menzel[1]

[1]GE Global Research, Munich, Germany, [2]Technical University Munich, Munich, Germany, [3]GE Healthcare, Munich, Germany, [4]GE Global Research, Niskayuna, NY, United States, [5]Max Planck Institute of Psychiatry, Munich, Germany

Introduction: The study of diffusion properties by MRI methods has gained significant importance for understanding the central nervous system [1]. The conventional DTI model is based on a Gaussian diffusion model, which assumes a linear dependence of the b-value and the signal attenuation in the radial direction. Jensen et al. introduced diffusional kurtosis imaging (DKI) to describe the broadening or compression of the propagator function in biological tissue due to barriers (e.g. membranes) and compartments (e.g. intracellular and extracellular spaces) [2]. The typical acquisition scheme for DKI comprises 150 points equally distributed to 5 shells in the diffusion encoding space (q-space). Alternatively, Poot et. al proposed a 3-shell acquisition with an increasing number of sampling points per shell which has been shown to provide better efficiency [3]. However the major problem in DKI still is a low SNR of the data. Recently a new technique, called compressed-sensing-accelerated diffusion spectrum imaging (CS-DSI) [4] has been developed which exploits the sparsity in the Total Variation (TV) and wavelet domain to denoise the data and reconstruct the full q-space. In this work we optimized the acquisition and reconstruction parameters of CS-DSI for DKI and compared the results with the standard kurtosis acquisition techniques.

Theory: In an undersampled DSI experiment the CS approach [4] reconstructs the data *x* in the reciprocal *r-space* by solving

$$\min_x \|Ax - y\|_2 + \lambda\|\Psi x\|_1 + \mu\|\Omega x\|_1 \qquad (1)$$

with *y* the undersampled q-space data, *A=MF* (undersampling operator and Fourier transform), Ψ a sparsifying transform into total variation domain, Ω a sparsifying transform into wavelet domain and λ and μ the corresponding weights. Eq. 1 can be solved using standard iterative shrinkage/thresholding algorithms (ISTA) [5].

Methods: Echo-planar DSI experiments were performed on one healthy volunteer using a 3T GE MR750 MR scanner (GE Healthcare, Waukesha, WI, USA), equipped with a 32 channel head coil (TE=80.7ms, TR=2s, 96x96, FOV=24 cm, 16 slices, slice=2.5 mm, ASSET factor 2, b_{max}=3,000 s/mm²). Different q-space acquisition schemes were acquired (see Fig. 1): a) 10 repetitions of standard acquisition scheme, i.e. 5 shells (b_{max}=600, 1200, 1800, 2400, 3000 s/mm²) with 30 directions per shell, b) 3 shells (b_{max}=750, 1070, 3000 s/mm²) with 25, 40, 75 directions, respectively, [3], and c) undersampled 11x11x11 DSI where 150 points are uniform randomly sampled within a sphere. In addition, b=0-images were acquired every 20th image and used for affine motion correction. A gold standard was calculated by averaging 9 repetitions of acquisition scheme a). The undersampled DSI data of acquisition scheme c) was reconstructed to full q-space data using CS with empirically optimized weights for TV and wavelet constraints. The diffusion and kurtosis tensor was fitted to the data using weighted linear least squares fitting (WLLS) with constraints ensuring positive apparent diffusion coefficients (ADC) as well as positive apparent kurtosis coefficients (AKC). For the comparison of the different acquisition schemes, scalar metrics like mean kurtosis, maximum kurtosis and radial kurtosis as well as the AKC for 256 equally distributed directions were calculated.

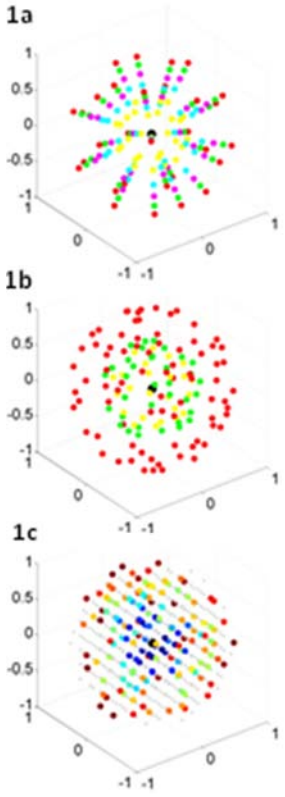

Results: Fig. 2 depicts error histograms with respect to the gold standard for a) maximum kurtosis and b) radial kurtosis for one exemplary data set. The error histogram of the CS reconstructed data is narrower and higher than the histogram of the undersampled as well as the 5 shell dataset and comparable to the 3 shell acquisition scheme. Fig. 3 shows the resulting scalar kurtosis measures as well as the RMSE of the AKC for a representative slice. The maps based on the CS reconstructed data appear less noisy without losing structural information compared to the 5-shell and 3-shell acquisition schemes, especially for unstable metrics like radial kurtosis. Furthermore the RMSE of the AKC is reduced.

Discussion: The combination of CS-DSI and kurtosis imaging showed a superior quality of kurtosis maps with respect to the most common 5-shell acquisition scheme as well as the 3-shell acquisition scheme. Furthermore the reconstruction of full q-space enables the option to calculate the r- space by simple Fourier transform which can be used for ODF based fiber tracking or other fitting models.

2a)

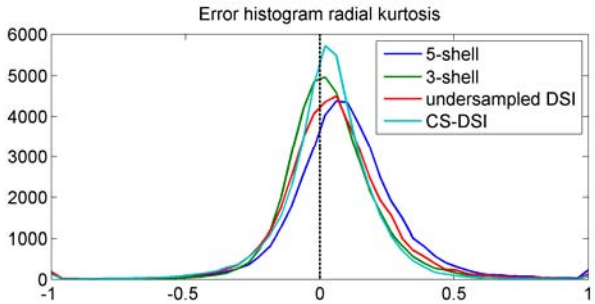

2b)

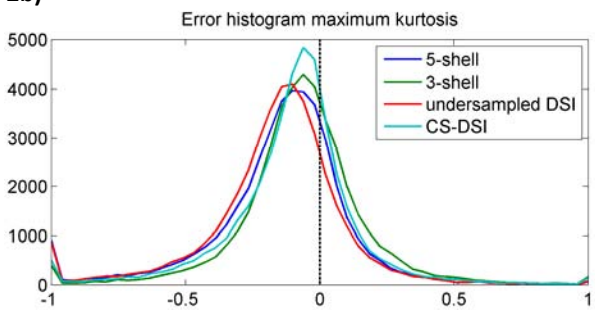

3)

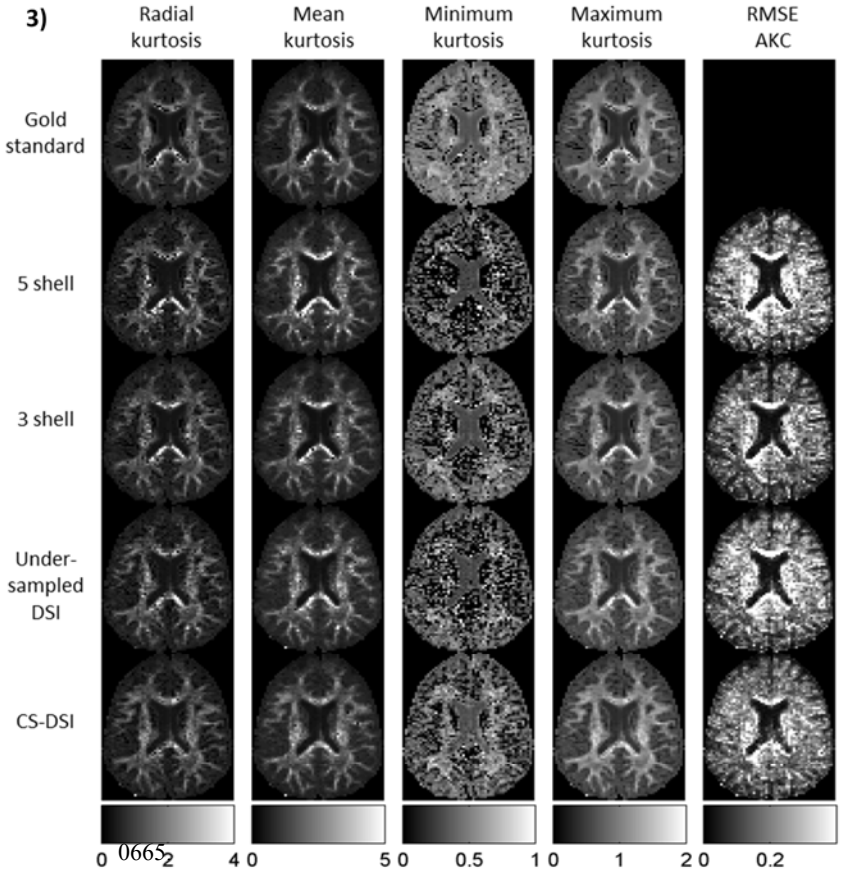

References:

[1] Baker et. al, Neuroscience & Biobehavioral Reviews. 2013; 37(8) : 1713–1723

[2] Jensen, J.H. and J.A. Helpern, NMR Biomed. 2010, 23(7):698-710

[3] Poot et. al, Trans Med Imaging 2010 Mar; 29(3) :819-29

[4] Menzel et. al, MagnReson Med. 2011;66(5):1226-33

[5] Daubechies, Ingrid, et al. Comm. Pure Appl. Math. 57.11 (2004): 1413–1457.